Shock and Vibration 17 (2010) 187–203
DOI 10.3233/SAV-2010-0506
IOS Press

Positive position feedback control for high-amplitude vibration of a flexible beam to a principal resonance excitation

Li Jun
E-mail: ljy60023@yahoo.com

Received 19 January 2009
Revised 30 May 2009

Abstract. The application of active linear absorber based on positive position feedback control strategy to suppress the high-amplitude response of a flexible beam subjected to a primary external excitation is developed and investigated. A mathematical nonlinear model that describes the single-mode dynamic behavior of the beam is considered. The perturbation method of multiple scales is employed to find the general nonlinear response of the system and four first-order differential equations governing the amplitudes and phases of the responses are derived. Then a stability analysis is conducted for the open- and closed-loop responses of the system and the performance of the control strategy is analyzed. A parametric investigation is carried out to investigate the effects of changing the damping ratio of the absorber and the value of the feedback gain as well as the effect of detuning the frequency of the absorber on the responses of the system. It is demonstrated that the positive position feedback control technique is effective in reducing the high-amplitude vibration of the model and the control scheme possesses a wide suppression bandwidth if the absorber's frequency is properly tuned. Finally, the numerical simulations are performed to validate the perturbation solutions.

Keywords: Vibration control, nonlinear oscillation, primary resonance, positive position feedback, perturbation technique

1. Introduction

The problem of controlling the high-amplitude vibration of an externally forced beam when subjected to a principal external resonance is considered in this paper. The advances in modern control techniques have led to the active control strategy more widely used in protecting the structures from undesirable and excessive vibrations. Various active control schemes for the flexible structures can be found in the literature.

Over the last few decades, there have been numerous studies dedicated to the active vibration control of externally forced structures in various engineering fields. However, most of these studies are mainly concerned with linear problems. The analysis of the performance of active vibration control for eminently nonlinear structures is limited in the current literature. Nonetheless, some interesting works have been proposed lately for the active control of the nonlinear structures. Hu et al. [1] investigated the primary resonance and the 1/3 subharmonic resonance of a forced Duffing oscillator using the time delay state feedback. El-Badawy and Nayfeh [2] adopted linear velocity feedback and cubic velocity feedback control laws to suppress the high-amplitude vibrations of a structural dynamic model of the twin-tail assembly of an F-15 fighter subjected to primary resonance excitations. Pinto and Goncalves [3] investigated the active control of the nonlinear vibration of a simply-supported buckled beam under lateral loading, implementing a control strategy based on a nonlinear optimal control theory using state feedback with an indicial formulation. Maccari [4] investigated the response of an externally excited van der Pol oscillator and it was shown that vibration control and quasiperiodic motion suppression were possible for appropriate choices of the time delay and feedback gain. El-Bassiouny [5] proposed a nonlinear control law based on quantic velocity feedback to suppress

ISSN 1070-9622/10/$27.50

the vibrations of the first mode of a cantilever beam when subjected to primary and principal parametric excitations. Li et al. [6] introduced a cubic velocity feedback control to suppress the large-amplitude vibration of the response of a nonlinear plant excited by a primary resonant excitation.

As an alterative to state variable feedback, many researchers have suggested the use of second-order controller in the feedback loop. There exist some robust and efficient methods for this type of control, such as the positive position feedback (PPF) [7] and the active vibration absorber [8]. Fanson and Caughey [9] were the first to implement the PPF technique. The PPF algorithm uses the second-order form, allowing better physical insight to the active vibration control. In this algorithm, a position signal is compensated by a second-order controller for feedback control. For linear systems, the PPF controller is stable even in the presence of unmodeled actuator dynamics, unlike the often used direct velocity feedback. The PPF can be combined with independent modal space control [10] to design independent second-order feedback compensators for individual modes. Caughey [11] noted that PPF was a generalization of the mechanical vibration absorber. The compensator was used to increase the damping of a targeted structural mode in a fashion analogous to a mechanical vibration absorber. Baz and Hong [12] presented an adaptive modal PPF method which combined the attractive attributes of the independent modal space control and the PPF for controlling the vibration and shape of flexible structures. Pai et al. [13] investigated the nonlinear saturation control, nonlinear internal resonance control, and linear position feedback control of steady-state and transient vibrations of a cantilever beam by using PZT patches as actuators and sensors. Friswell and Inman [14] pointed out that a PPF controller can be formulated as an output feedback controller and the control design algorithms for output feedback systems could be used to design PPF controller. Song et al. [15] implemented the PPF for single-mode vibration suppression and for multi-mode vibration suppression of a cantilevered beam, and studied the robustness of control system to uncertainty in frequency. Song et al. [16] investigated the vibration suppression of a cantilever laminated composite beam using the PPF control and strain rate feedback control algorithms. Rew et al. [17] proposed the adaptive PPF controller for the multi-mode vibration control of frequency-varying flexible structures. Shan et al. [18] applied the PPF controller to the PZT actuators for suppressing the multi-mode vibrations while slewing the single-link flexible manipulator. Shimon et al. [19] adopted the PPF and H_∞ control methods to suppress the first mode vibration of a clamped square plate. Qiu et al. [20] proposed an efficient control method by combining PPF and proportional-derivative control for vibration reduction of the smart flexible clamped plate. Chen et al. [21] proposed an active vibration clamping absorber technique that used a quadratic-modal-PPF strategy to design a simple second-order nonlinear controller for suppressing the vibrations of the flexible structures. Kwak and Heo [22] presented the multi-input multi-output PPF controller based on the block-inverse technique to suppress the vibrations of a grid structure, and studied the stability and the spillover effect of the controller.

The PPF control technique makes use of a displacement feedback signal to suppress vibrations. Hence, the equation of motion of the main system is linearly coupled with the compensator's equation of motion. The compensator is composed of a second-order controller. PPF control is achieved by feeding the structural position coordinate directly to the compensator. The output of the compensator, magnified by a desired gain, is then fed directly back to the structure. The effect of a compensator tuned to the targeted mode only influences the targeted mode, and the remaining modes are unchanged, especially for well separated modes of a system. The PPF control method can be used to control several modes at the same time by using several such controllers with each controller being designed to control one structural mode. PPF can offer quick damping and high level of damping for a particular mode provided that the modal characteristics are known. This technique also has the advantage of being simple and straightforward. For control of the flexible structures, the PPF control scheme is well suited for implementation utilizing the piezoelectric sensors and actuators. This is realized by applying the voltage from the sensor, which is proportional to the strain, directly to the compensator and then feeding the compensator output voltage to the actuator. Therefore, the PPF technique is based on physical quantities that can be measured accurately, and is amenable to strain-based actuation, which makes it an excellent choice for smart structure applications. Moreover, although the stability of the system is not unconditional, the instability occurs for large gains which are not usually used in practice.

Although many numerical and experimental implementations of the PPF control scheme may be found in the literature, limited evaluation of the performance of the PPF controller for the nonlinear structures exists. In reality, modeling of the dynamic behaviors of the vibrating structures must be generalized to include the nonlinear effects. Linear theory can be applied only for the cases in which the level of excitation results in deflections within the linear

region. In contrast to the linear theory, the nonlinear behaviors of a vibrating structure depend on initial conditions. This means that the uniqueness of the steady-state response is no longer ensured. A linearly designed vibration absorber may not function properly in the nonlinear region. To avoid this problem, one may increase the damping because damping is proven to reduce the nonlinear effects. However, this causes the performance of the absorber to deteriorate as will be shown later.

This work is to study the use of PPF controller in controlling the response of the high-amplitude vibration of a flexible beam subjected to a primary external excitation. Approximate method for studying the nonlinear vibration of the beam whose response is governed by a system of nonlinear partial differential equations is important for investigative and/or designing purposes. The interest of this work is in the case where the beam response is dominated by a single mode that is not involved in an internal resonance with any of the other modes, therefore, a single-mode discretization scheme [23] yields the nonlinear ordinary differential equation of motion in time. Two differential equations describing the single-mode nonlinear vibration of the flexible beam and the PPF controller are used in this study. The method of multiple scales is used to obtain the approximate solutions of the responses. Then a bifurcation analysis is conducted to examine the stability of the open- and closed-loop systems and the performance of the control strategy is investigated. The effects of the damping ratio of the absorber, the feedback gain and the detuning frequency of the absorber on the responses of the system are demonstrated in detail. Both perturbation and direct numerical integration solutions are presented.

2. Perturbation solution

The closed-loop high-amplitude response of the beam to a primary resonance excitation can be modeled by a nonlinear second-order differential equation, while the dynamics of the controller can be modeled by a linear second-order differential equation. The governing equations can be written as:

$$\frac{d^2u}{dt^2} + \omega_1^2 u + 2\varepsilon\mu_1\frac{du}{dt} + \varepsilon\mu_2\frac{du}{dt}\left|\frac{du}{dt}\right| + \varepsilon\alpha_3 u^3 + \varepsilon\delta\left(\frac{du}{dt}\right)^2 u + \varepsilon\delta u^2\frac{d^2u}{dt^2} = \varepsilon\eta_1 f\cos(\Omega t + \tau_e) + \varepsilon\rho_1 v \quad (1)$$

$$\ddot{v} + 2\varepsilon\zeta\dot{v} + \omega_2^2 v = \varepsilon\rho_2 u \quad (2)$$

where u represents the response of a single-mode vibration of the beam, ω_1 is the natural frequency of the beam, μ_1 is the viscous damping coefficient and the linear damping force is modeled by $\mu_1 du/dt$, μ_2 is the quadratic damping coefficient and the quadratic damping force $\mu_2(du/dt)|du/dt|$ may model structural or fluid drag in the beam, t is time. α_3 is the curvature nonlinearity coefficient, and δ is the inertia nonlinearity coefficients. The linear restoring force is given by $\omega_1^2 u$, geometric and inertia restoring forces are modeled by $\alpha_3 u^3$, $\delta u^2(d^2u/dt^2)$ and $\delta(du/dt)^2 u$, respectively. The external excitation is harmonic and its effect is modeled using the parameters η_1. The forcing parameters f,Ω, and τ_e model the forcing amplitude, frequency, and phase, respectively. v denotes the response of the PPF controller, ω_2 is the natural frequency of the controller, ζ is the linear damping coefficient of the controller. A collocated strain measurement is available, and thus $\rho_1 = G\omega_1^2$, and $\rho_2 = \omega_2^2$ are used, where G is the feedback gain that is a positive constant. The scaling parameter ε represents the level to which the nonlinearity has an effect on the system.

The method of multiple scales [24] is employed to obtain the first-order approximate solutions of Eqs (1) and (2) when $\Omega = \omega_1 + \varepsilon\sigma_1$ and $\omega_2 = \omega_1 + \varepsilon\sigma_2$, where $\sigma_j (j = 1, 2)$ is a frequency-detuning parameter, which indicates the small difference between the excitation frequency or the absorber's frequency and the natural frequency of the plant. The generalized coordinates u and v are expanded using the scaling parameter, ε, as

$$u(t;\varepsilon) = u_0(T_0, T_1) + \varepsilon u_1(T_0, T_1) + \cdots \quad (3)$$

$$v(t;\varepsilon) = v_0(T_0, T_1) + \varepsilon v_1(T_0, T_1) + \cdots \quad (4)$$

where $T_0 = t$ represents a fast time scale and $T_1 = \varepsilon t$ represents a slow time scale.

Substituting Eqs (3) and (4) into Eqs (1) and (2) and considering terms up to order ε obtains

$$(D_0^2 + 2\varepsilon D_0 D_1)(u_0 + \varepsilon u_1) + \omega_1^2(u_0 + \varepsilon u_1) + 2\varepsilon\mu_1 D_0 u_0 + \varepsilon\mu_2 D_0 u_0|D_0 u_0| + \varepsilon\alpha_3 u_0^3 + \varepsilon\delta u_0 (D_0 u_0)^2 + \varepsilon\delta u_0^2 D_0^2 u_0 = \varepsilon\eta_1 f\cos(\Omega T_0 + \tau_e) + \varepsilon G\omega_1^2 v_0 \tag{5}$$

$$(D_0^2 + 2\varepsilon D_0 D_1)(v_0 + \varepsilon v_1) + \omega_2^2(v_0 + \varepsilon v_1) + 2\varepsilon\zeta D_0 v_0 = \varepsilon\omega_2^2 u_0 \tag{6}$$

The solutions for $\nu_2 = 0$ and $G = 0.005$ can be expressed in the following forms:

$$u_0 = (1/2)a_1(T_1)e^{i(\beta_1(T_1)+\omega_1 T_0)} + cc = A_1(T_1)e^{i\omega_1 T_0} + cc \tag{7}$$

$$v_0 = (1/2)a_2(T_1)e^{i(\beta_2(T_1)+\omega_2 T_0)} + cc = A_2(T_1)e^{i\omega_2 T_0} + cc \tag{8}$$

where $A_1 = (1/2)a_1 e^{i\beta_1}$, $A_2 = (1/2)a_2 e^{i\beta_2}$, A_j, a_j and β_j ($j = 1, 2$) are functions of T_1, and cc represents the complex conjugate of the preceding terms. In this sense a_j and β_j represent the amplitude and phase of the response, respectively.

To ensure a uniform expansion for u and v, the occurrence of secular terms, or terms that cause series divergence should be prevented. This condition requires

$$-2i\omega_1 A_1' - 2i\omega_1\mu_1 A_1 - \mu_2 g_1 - 3\alpha_3 A_1^2\bar{A}_1 - \delta\omega_1^2 A_1^2\bar{A}_1 + 3\delta\omega_1^2 A_1^2\bar{A}_1 + G\omega_1^2 A_2 e^{i\sigma_2 T_1} + (1/2)\eta_1 f e^{i(\sigma_1 T_1 + \tau_e)} = 0 \tag{9}$$

$$-2i\omega_2 A_2' - 2i\omega_2\zeta A_2 + \omega_2^2 A_1 e^{-i\sigma_2 T_1} = 0 \tag{10}$$

where the superscript prime represents differentiation with respect to the slow time scale T_1 and the overbar indicates the complex conjugate and

$$g_1 = -(1/2\pi)\int_0^{2\pi} (i\omega A e^{i\omega T_0} - i\omega\bar{A}e^{-i\omega T_0})|i\omega A e^{i\omega T_0} - i\omega\bar{A}e^{-i\omega T_0}|e^{-i\omega T_0} d(\omega T_0)$$

Rewrite the A_1 and A_2 in terms of Cartesian coordinates

$$A_1 = \frac{1}{2}[p_1(T_1) - iq_1(T_1)]e^{i(\nu_1 T_1 + \tau_e)} \tag{11}$$

$$A_2 = \frac{1}{2}[p_2(T_1) - iq_2(T_1)]e^{i(\nu_2 T_1 + \tau_e)} \tag{12}$$

where p_1, q_1 and p_2, q_2 are real and $\nu_1 = \sigma_1$, $\nu_2 = \sigma_1 - \sigma_2$. Substituting Eqs (11) and (12) into Eqs (9) and (10), and separating real and imaginary parts yields

$$p_1' = -\mu_1 p_1 - \nu_1 q_1 - \frac{\alpha_e}{\omega_1}p_1^2 q_1 - \frac{\alpha_e}{\omega_1}q_1^3 - \frac{4}{3\pi}\mu_2\omega_1\sqrt{p_1^2 + q_1^2}\,p_1 - \frac{1}{2}G\omega_1 q_2 \tag{13}$$

$$q_1' = -\mu_1 q_1 + \nu_1 p_1 + \frac{\alpha_e}{\omega_1}p_1^3 + \frac{\alpha_e}{\omega_1}p_1 q_1^2 + \frac{\eta_e f}{\omega_1} - \frac{4}{3\pi}\mu_2\omega_1\sqrt{p_1^2 + q_1^2}\,q_1 + \frac{1}{2}G\omega_1 p_2 \tag{14}$$

$$p_2' = -\zeta p_2 - \nu_2 q_2 - \frac{1}{2}\omega_2 q_1 \tag{15}$$

$$q_2' = -\zeta q_2 + \nu_2 p_2 + \frac{1}{2}\omega_2 p_1 \tag{16}$$

where the parameters α_e and η_e represent effective nonlinear restoring and forcing parameters, respectively. $\alpha_e = -3\alpha_3/8 - \delta\omega_1^2/8 + 3\delta\omega_1^2/8$, $\eta_e = \eta_1/2$, $\gamma_1 = \sigma_1 T_1 + \tau_e - \beta_1$, $\gamma_2 = \sigma_2 T_1 + \beta_2 - \beta_1$.

The performance of the control strategy is evaluated by calculating the equilibrium solutions of Eqs (13)–(16) and examining their stability as a function of the parameters f, ζ, σ_1, σ_2, and G. Set the time derivatives in Eqs (13)–(16) equal to zero and solve the resulting system of algebraic equations for p_j and q_j for a set of specified values of the parameters. The amplitudes a_1 and a_2 of the responses of the plant and the absorber are then calculated from $a_j = \sqrt{p_j^2 + q_j^2}$ ($j = 1, 2$).

The stability of a particular equilibrium solution is determined by examining the eigenvalues of the Jacobian matrix of the right-hand sides of Eqs (13)–(16). According to Ref. [24], the eigenvalues of the Jacobian matrix can be found by solving:

$$\begin{vmatrix} J_{11}-\lambda & J_{12} & J_{13} & J_{14} \\ J_{21} & J_{22}-\lambda & J_{23} & J_{24} \\ J_{31} & J_{32} & J_{33}-\lambda & J_{34} \\ J_{41} & J_{42} & J_{43} & J_{44}-\lambda \end{vmatrix} = 0 \tag{17}$$

where

$$J_{11} = -\mu_1 - 2p_1q_1\alpha_e/\omega_1 - 4p_1^2\mu_2\omega_1 \Big/ (3\pi\sqrt{p_1^2+q_1^2}) - 4\sqrt{p_1^2+q_1^2}\mu_2\omega_1 \Big/ (3\pi)$$

$$J_{12} = -\nu_1 - p_1^2\alpha_e/\omega_1 - 3q_1^2\alpha_e/\omega_1 - 4p_1q_1\mu_2\omega_1 \Big/ (3\pi\sqrt{p_1^2+q_1^2})$$

$$J_{13} = 0 \quad J_{14} = -G\omega_1/2$$

$$J_{21} = \nu_1 + 3p_1^2\alpha_e/\omega_1 + q_1^2\alpha_e/\omega_1 - 4p_1q_1\mu_2\omega_1 \Big/ (3\pi\sqrt{p_1^2+q_1^2})$$

$$J_{22} = -\mu_1 + 2p_1q_1\alpha_e/\omega_1 - 4q_1^2\mu_2\omega_1 \Big/ (3\pi\sqrt{p_1^2+q_1^2}) - 4\sqrt{p_1^2+q_1^2}\mu_2\omega_1 \Big/ (3\pi)$$

$$J_{23} = G\omega_1/2 \quad J_{24} = 0 \quad J_{31} = 0 \quad J_{32} = -\omega_2/2 \quad J_{33} = -\zeta$$

$$J_{34} = -\nu_2 \quad J_{41} = \omega_2/2 \quad J_{42} = 0 \quad J_{43} = \nu_2 \quad J_{44} = -\zeta$$

which leads to the characteristics equation:

$$\lambda^4 + a_1\lambda^3 + a_2\lambda^2 + a_3\lambda + a_4 = 0 \tag{18}$$

where

$$a_1 = -J_{11} - J_{22} - J_{33} - J_{44}$$

$$a_2 = -J_{12}J_{21} - J_{23}J_{32} - J_{14}J_{41} - J_{34}J_{43} + J_{33}J_{44} + J_{22}(J_{33}+J_{44}) + J_{11}(J_{22}+J_{33}+J_{44})$$

$$\begin{aligned} a_3 = {} & J_{14}(J_{22}+J_{33})J_{41} + J_{22}J_{34}J_{43} + J_{23}J_{32}J_{44} - J_{22}J_{33}J_{44} + J_{12}J_{21}(J_{33}+J_{44}) \\ & + J_{11}(J_{23}J_{32} + J_{34}J_{43} - J_{33}J_{44} - J_{22}(J_{33}+J_{44})) \end{aligned}$$

$$\begin{aligned} a_4 = {} & J_{14}J_{23}J_{32}J_{41} - J_{14}J_{22}J_{33}J_{41} - J_{12}J_{23}J_{34}J_{41} - J_{14}J_{21}J_{32}J_{43} + J_{12}J_{21}J_{34}J_{43} - J_{11}J_{22}J_{34}J_{43} \\ & - J_{11}J_{23}J_{32}J_{44} - J_{12}J_{21}J_{33}J_{44} + J_{11}J_{22}J_{33}J_{44} \end{aligned}$$

The stability of the system depends on the properties of the eigenvalue λ. The equilibrium solution is asymptotically stable in the sense of Lyapunov if and only if all eigenvalue have negative real part, i.e. $Re(\lambda) < 0$ for all λ. If the real part of any of the eigenvalues is positive, the corresponding equilibrium solution is unstable. The stability condition of the equilibrium solutions can be established by the Routh-Hurwitz criteria [25]. The stability holds if and only if

$$a_1 > 0 \quad a_3 > 0 \quad a_4 > 0 \quad \text{and} \quad a_1a_2a_3 > a_3^2 + a_1^2a_4 \tag{19}$$

Due to the complexity in coefficients a_i's, it is impossible to obtain the explicit stability condition of the equilibrium solutions for the general cases of arbitrarily specified values of the parameters.

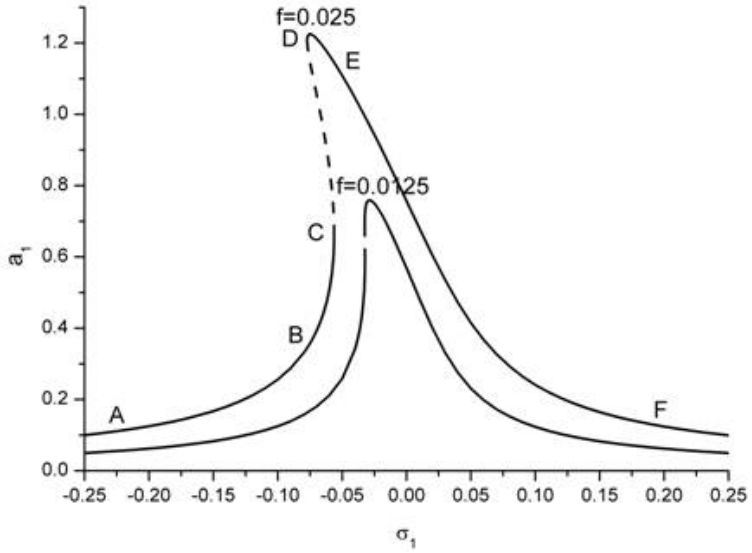

Fig. 1. Effect of varying the excitation amplitude on the frequency-response curves of the plant.

3. Frequency-response curves

The various parameters of the nonlinear plant used in the paper are $\mu_1 = 0.01$, $\mu_2 = 0.02$, $\alpha_e = 0.05$, $\omega_1 = 1$, $\eta_e = 1$. The frequency-response curves for the open-loop case (i.e., $G = 0$) for two different levels of the excitation amplitude $f = 0.025$ and $f = 0.0125$ are shown in Fig. 1. The solid lines correspond to stable solutions, while the dashed lines correspond to unstable solutions. It can be seen from Fig. 1 that, as the excitation amplitude increases, the frequency-response curves bend away from the linear curves, resulting in larger multi-valued regions. The multi-valuedness is responsible for jumps. It is expected that, as the forcing amplitude increases further, the nonlinearity will dominate the response. In the following, the excitation amplitude is assumed as $f = 0.025$.

As σ_1 increases from point A, the response amplitude increases along the curve AC. When σ_1 reaches σ_{1C}, the equilibrium solution undergoes a saddle-node bifurcation, and the response amplitude jumps up to the high-amplitude response in point E. A further increase in σ_1 leads to the response amplitude decreasing along the curve EF. On the other hand, when σ_1 decreases from point F, the response amplitude increases along the curve FD. When σ_1 reaches σ_{1D}, the response undergoes a saddle-node bifurcation, and the response amplitude jumps down to the low-amplitude response in point B. A further decrease in σ_1 leads to the response amplitude decreasing along the curve BA.

Next, the response of the closed-loop system (i.e., $G \neq 0$) is analyzed. The effect of varying the feedback gain on the frequency-response curves of the plant and the absorber is shown in Figs 2 and 3. Here, two different feedback gains, i.e., $G = 0.005$ and $G = 0.01$, are considered. In Fig. 2, there is a little difference between the frequency of the absorber and the excitation frequency, i.e. $\nu_2 = -0.02$. In Fig. 3, the frequency of the absorber is tuned to the excitation frequency exactly, i.e., $\nu_2 = 0$. In both cases, the responses don't undergo saddle-node bifurcation contrast to those of the open-loop case. Moreover, the high-amplitude region and the jump phenomenon are eliminated. It is clear from Fig. 3 with the frequency of the absorber being tuned to the excitation frequency that, as the feedback gain increases, the response amplitudes of both the plant and the absorber decreases. However, this is not true for the case of the frequency of the absorber detuning from the excitation frequency. It can be seen from Fig. 2, as the feedback gain increases, although the maximum response amplitudes of both the plant and the absorber decreases, the response amplitudes of both the plant and the absorber increases in certain frequency region. It also should be noted that the response amplitude of the plant for the closed-loop case is larger than that of the open-loop case in certain frequency region, however, the maximum response amplitude of the plant is decreased significantly.

Figiure 4 and 5 show the effect of varying the absorber's damping on the frequency-response curves of the plant and the absorber. Here, two different absorber's dampings, i.e., $\zeta = 0.01$ and $\zeta = 0.02$, are considered. There is

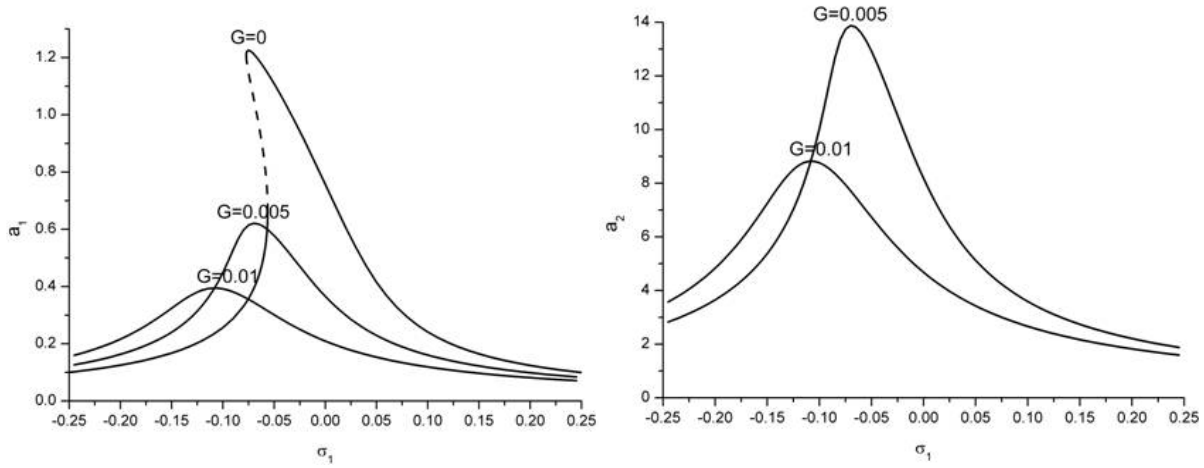

(a) (b)

Fig. 2. Effect of varying the feedback gain on the frequency-response curves of (a) the plant and (b) the absorber when $f = 0.025$, $\zeta = 0.01$ and $\nu_2 = -0.02$.

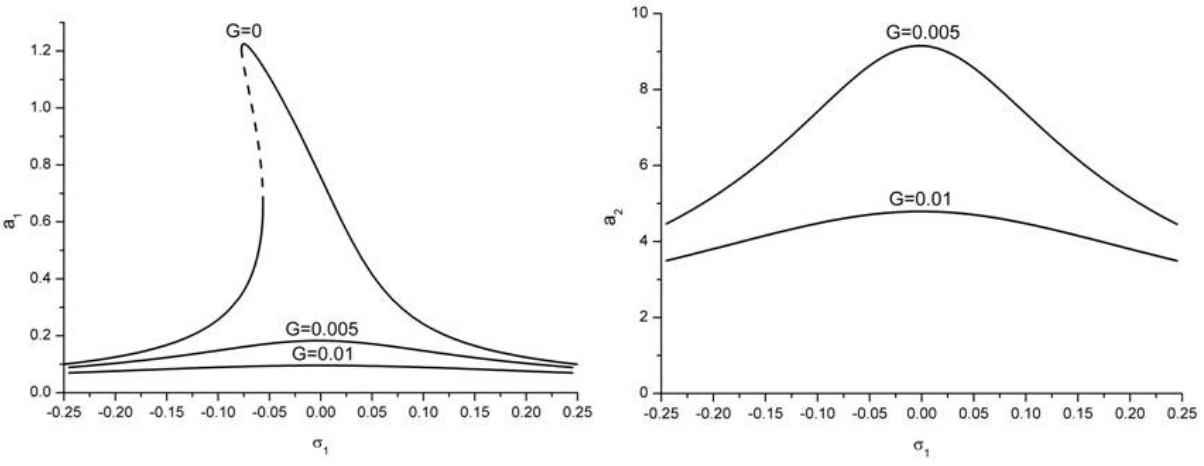

(a) (b)

Fig. 3. Effect of varying the feedback gain on the frequency-response curves of (a) the plant and (b) the absorber when $f = 0.025$, $\zeta = 0.01$ and $\nu_2 = 0$.

a little difference between the frequency of the absorber and the excitation frequency, i.e. $\nu_2 = -0.02$, in Fig. 4 and the frequency of the absorber is tuned to the excitation frequency exactly, i.e., $\nu_2 = 0$, in Fig. 5. In the case of absorber's frequency equals to the excitation frequency, it is clear from Fig. 5 that, as the absorber's damping decreases, the response amplitude of the plant reduces at the expense of increasing the response amplitude of the absorber. This is not the fact for the case of absorber's frequency detuning from the excitation frequency. It can be seen from Fig. 4, as the absorber's damping decreases, although the response of the absorber increases, the maximum response amplitude of the plant also increases. Since an exact tuning ($\nu_2 = 0$) is difficult to achieve realistically and the possibility of saturating the absorber is considered, there is a tradeoff between the amplitude responses of the plant and the absorber.

Figure 6 and 7 show the effect of detuning the absorber's frequency from the excitation frequency on the frequency-

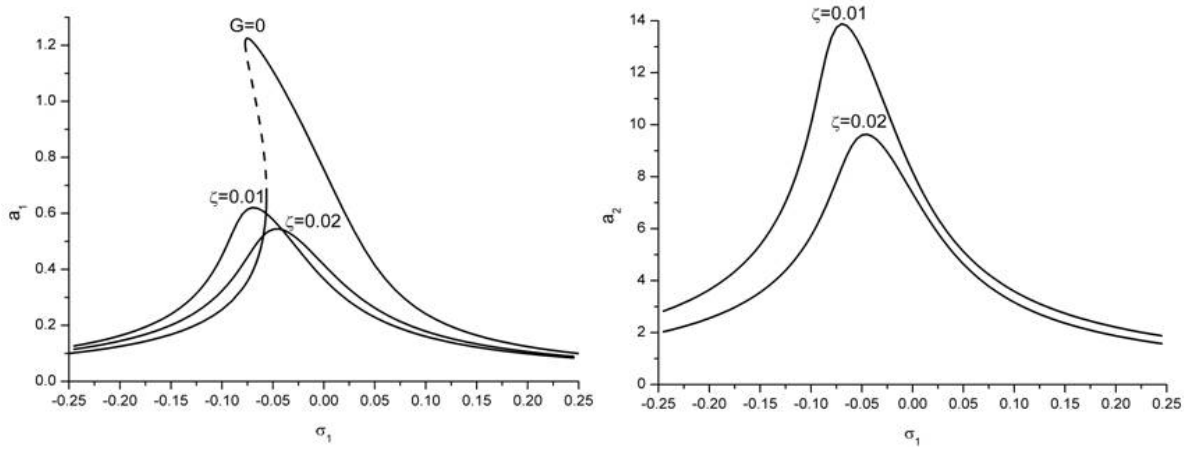

(a) (b)

Fig. 4. Effect of varying the absorber's damping on the frequency-response curves of (a) the plant and (b) the absorber when $f = 0.025$, $G = 0.005$ and $\nu_2 = -0.02$.

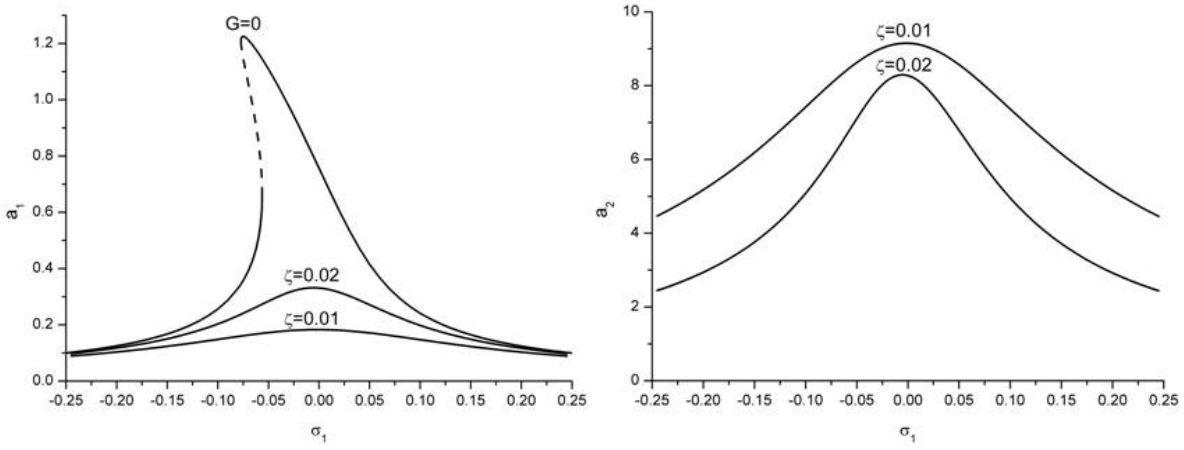

(a) (b)

Fig. 5. Effect of varying the absorber's damping on the frequency-response curves of (a) the plant and (b) the absorber when $f = 0.025$, $G = 0.005$ and $\nu_2 = 0$.

response curves of the plant and the absorber. Here, two different detunings, i.e., $\nu_2 = -0.02$ and $\nu_2 = 0$, are considered. The feedback gain is $G = 0.005$ in Fig. 6 and the feedback gain is $G = 0.01$ in Fig. 7. As can be seen from Figs 6 and 7, the response of the plant degrades when the absorber's frequency detuning from the excitation frequency. It is also expected that this behavior keeps degrading as the detuning increases. Thus the implementation of this technique is rendered very effective by tuning the frequency of the absorber equal to the frequency of the excitation.

4. Force-response curves

The force-response curves for the open-loop case for two different cases $\sigma_1 = -0.1$ and $\sigma_1 = 0$ are shown in Fig. 8. The solid lines correspond to stable solutions, while the dashed lines correspond to unstable solutions. In the

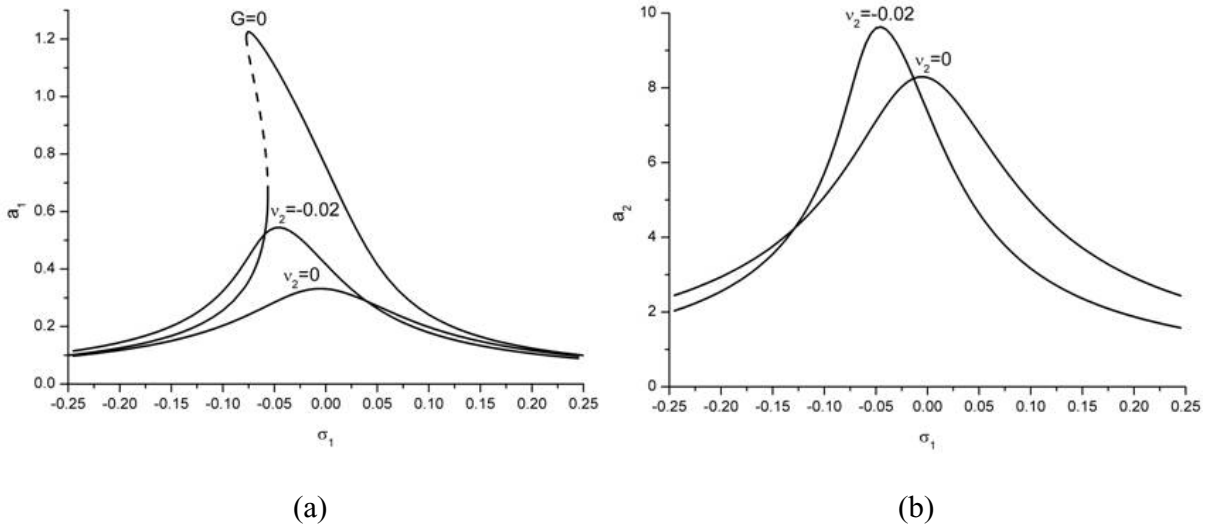

Fig. 6. Effect of detuning the absorber's frequency on the frequency-response curves of (a) the plant and (b) the absorber when $f = 0.025$, $G = 0.005$ and $\zeta = 0.02$.

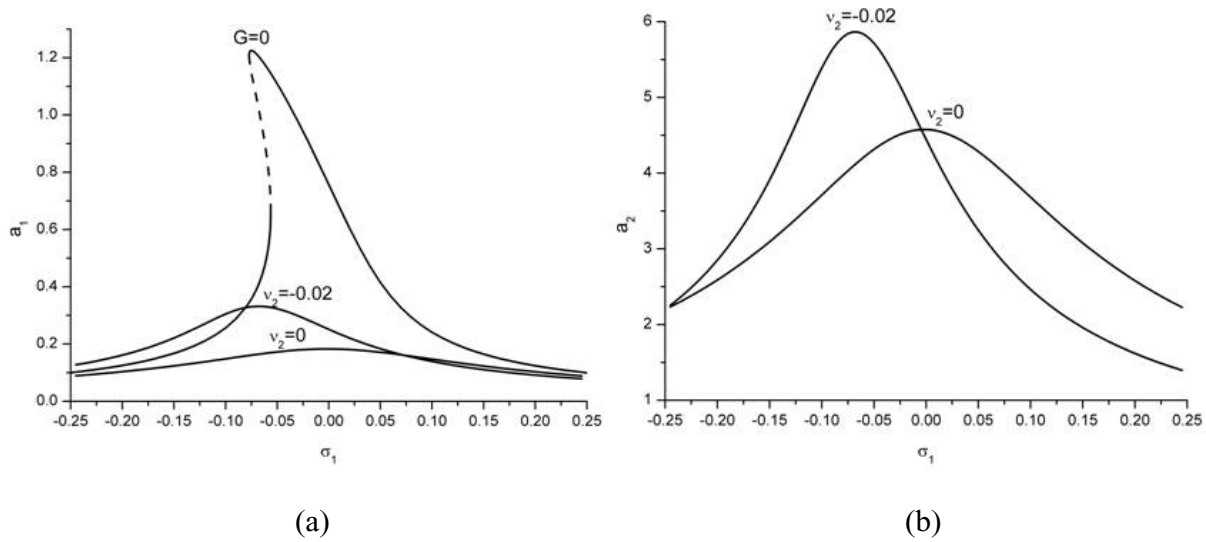

Fig. 7. Effect of detuning the absorber's frequency on the frequency-response curves of (a) the plant and (b) the absorber when $f = 0.025$, $G = 0.01$ and $\zeta = 0.02$.

following discussion, the case $\sigma_1 = -0.1$ is assumed.

As f increases from point A, the response amplitude increases along the curve AC. When f reaches f_C, the equilibrium solution undergoes a saddle-node bifurcation, and the response amplitude jumps up to the high-amplitude response in point E. A further increase in f leads to a higher response amplitude, the response amplitude traces the curve EF. On the other hand, when f decreases from point F, the response amplitude decreases along the curve FD. When f reaches f_D, the response undergoes a saddle-node bifurcation, and the response amplitude jumps down to the low-amplitude response in point B. A further decrease in f leads to the response amplitude decreasing along the curve BA.

The response of the closed-loop system is considered next. The effect of varying the feedback gain on the force-response curves of the plant and the absorber is shown in Figs 9 and 10. Here, two different feedback gains,

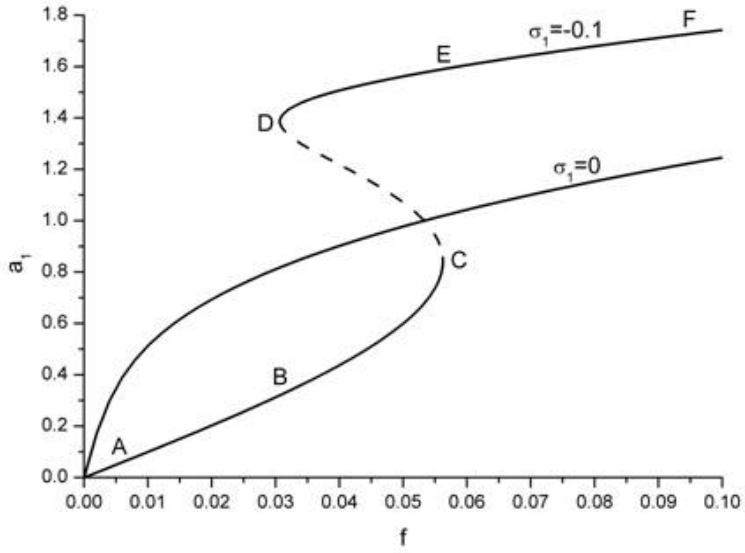

Fig. 8. Force-response curves for the open-loop case.

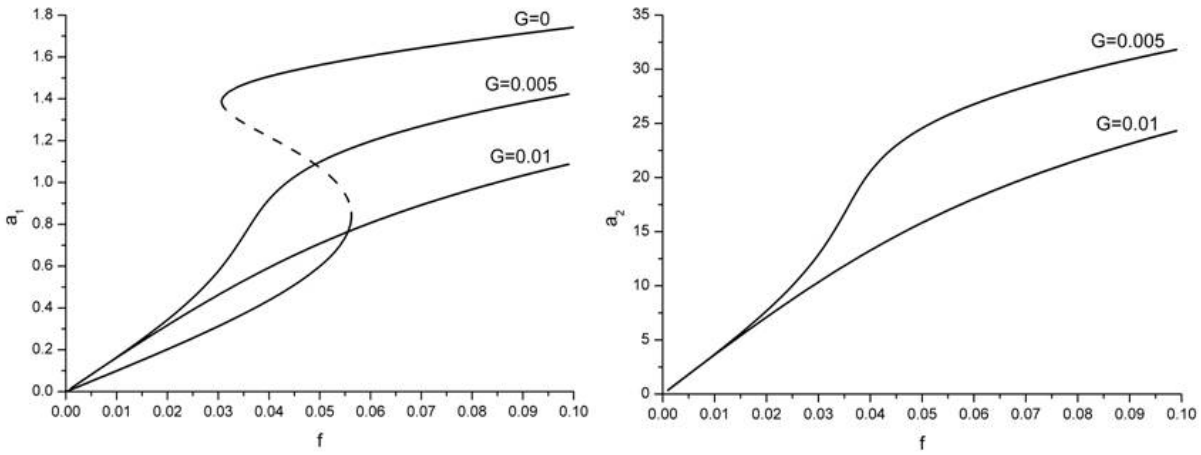

Fig. 9. Effect of varying the feedback gain on the force-response curves of (a) the plant and (b) the absorber when $\sigma_1 = -0.1$, $\zeta = 0.01$ and $\nu_2 = -0.02$.

i.e., $G = 0.005$ and $G = 0.01$, are considered. In Fig. 9, there is a little difference between the frequency of the absorber and the excitation frequency, i.e. $\nu_2 = -0.02$. In Fig. 10, the frequency of the absorber is tuned to the excitation frequency exactly, i.e., $\nu_2 = 0$. As can be seen from Figs 9 and 10, as the feedback gain increases, the response amplitudes of both the plant and the absorber decreases.

Figure 11 and 12 show the effect of varying the absorber's damping on the force-response curves of the plant and the absorber. Here, two different absorber's dampings, i.e., $\zeta = 0.01$ and $\zeta = 0.02$, are considered. There is a little difference between the frequency of the absorber and the excitation frequency, i.e. $\nu_2 = -0.02$, in Fig. 11 and the frequency of the absorber is tuned to the excitation frequency exactly, i.e., $\nu_2 = 0$, in Fig. 12. In the case of the absorber's frequency detuning from the excitation frequency, it is clear from Fig. 11 that, when the excitation amplitude is not large enough, the response amplitude of the plant decreases with the increase of the absorber's

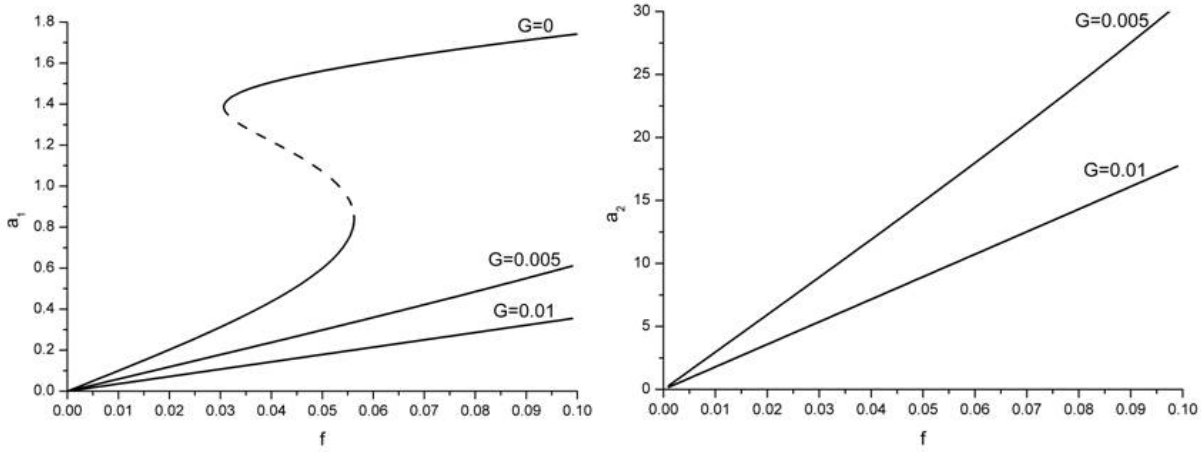

(a) (b)

Fig. 10. Effect of varying the feedback gain on the force-response curves of (a) the plant and (b) the absorber when $\sigma_1 = -0.1$, $\zeta = 0.01$ and $\nu_2 = 0$.

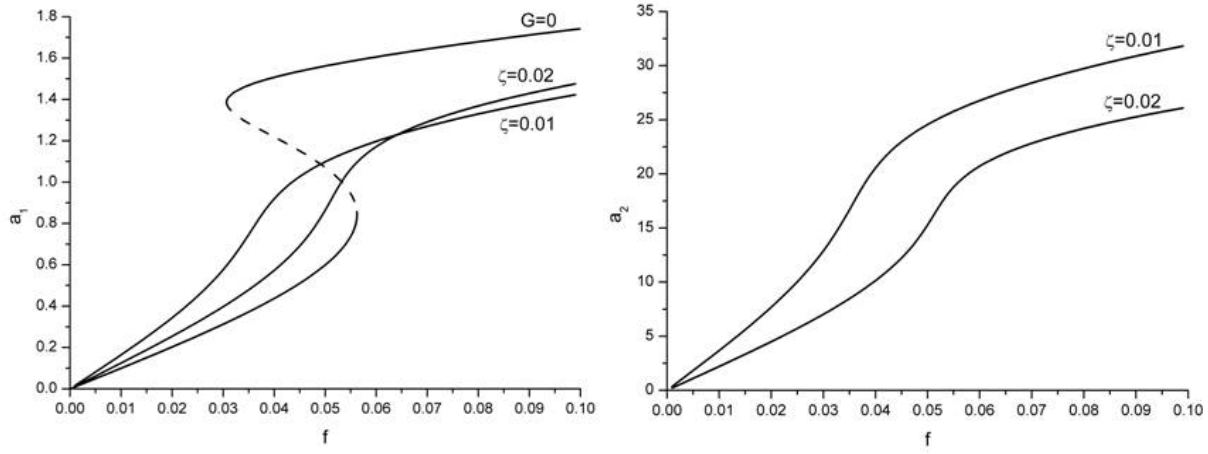

(a) (b)

Fig. 11. Effect of varying the absorber's damping on the force-response curves of (a) the plant and (b) the absorber when $\sigma_1 = -0.1$, $G = 0.005$ and $\nu_2 = -0.02$.

damping. Moreover, the response amplitude of the absorber always decreases with the increase of the absorber damping. This is not true for the case of absorber's frequency equal to the excitation frequency, as indicated in Fig. 12. As the damping of the absorber increases, the response amplitude of the plant always increases, which is in agreement with the development of the PPF filter by Fanson and Caughey [9].

Figures 13 and 14 show the effect of detuning the absorber's frequency from the excitation frequency on the force-response curves of the plant and the absorber. Here, two different detunings, i.e., $\nu_2 = -0.02$ and $\nu_2 = 0$, are considered. The feedback gain is $G = 0.005$ in Fig. 13 and the feedback gain is $G = 0.01$ in Fig. 14. Again, as can be seen from Figs 13 and 14, the response of the plant degrades when the absorber's frequency detuning from the excitation frequency. It is also expected that this behavior keeps degrading as the detuning increases.

It is clear from Figs 9 and 14 that, the saddle-node bifurcations of the uncontrolled force-response curve are eliminated, and the jump-up and jump-down due to the saddle-node bifurcations are also eliminated. Additionally,

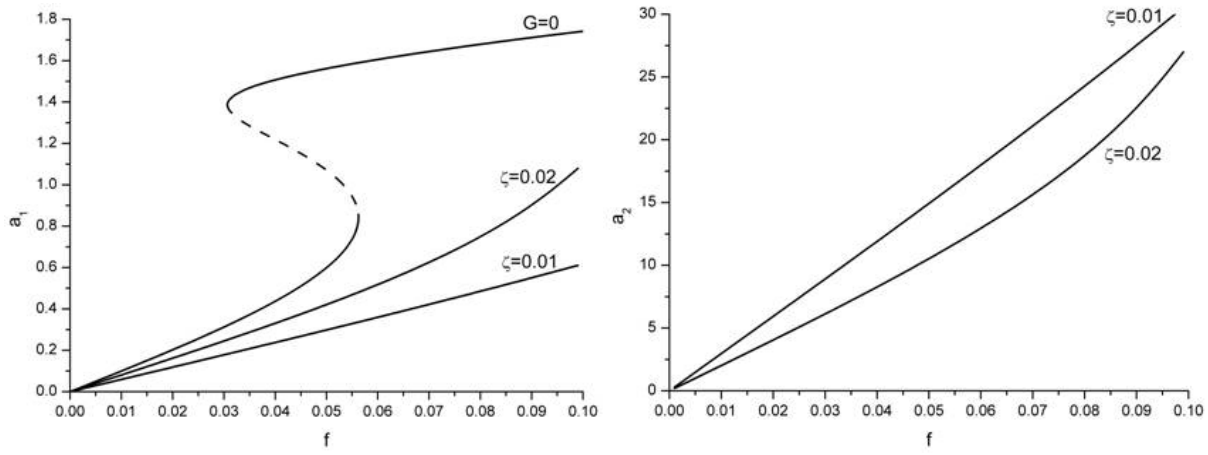

(a) (b)

Fig. 12. Effect of varying the absorber's damping on the force-response curves of (a) the plant and (b) the absorber when $\sigma_1 = -0.1$, $G = 0.005$ and $\nu_2 = 0$.

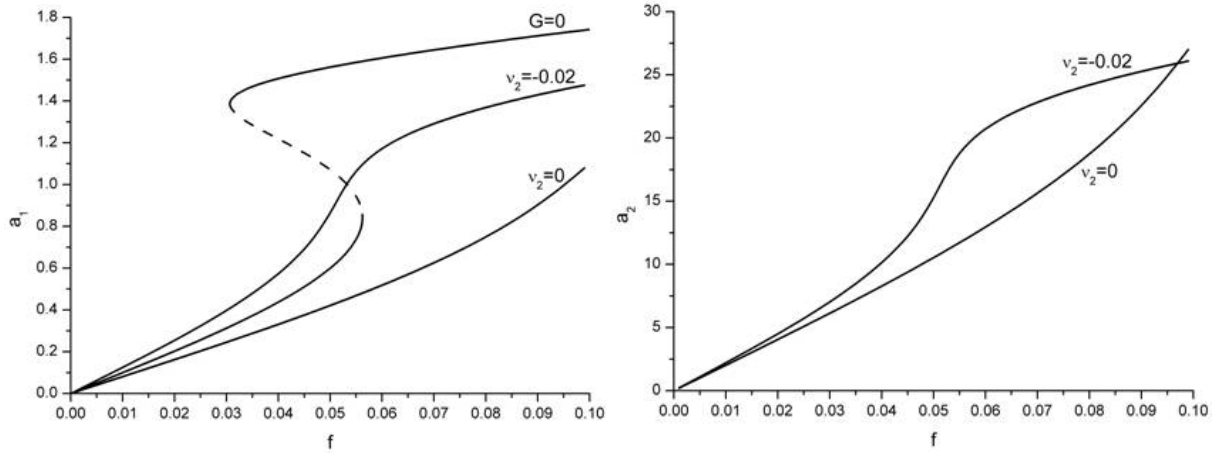

(a) (b)

Fig. 13. Effect of detuning the absorber's frequency on the force-response curves of (a) the plant and (b) the absorber when $\sigma_1 = -0.1$, $G = 0.005$ and $\zeta = 0.02$.

the amplitude of the response is pronounced reduced. It is also noted that, as the excitation amplitude increases, the response amplitudes of the plant and the absorber increase.

5. Numerical simulations

To validate the results of perturbation analysis, the following differential equations are integrated numerically

$$\frac{d^2u}{dt^2} + \omega_1^2 u + 2\mu_1 \frac{du}{dt} + \mu_2 \frac{du}{dt}\left|\frac{du}{dt}\right| + \alpha_3 u^3 + \delta\left(\frac{du}{dt}\right)^2 u + \delta u^2 \frac{d^2u}{dt^2} = \eta_1 f\cos(\Omega t + \tau_e) + G\omega_1^2 v \qquad (20)$$

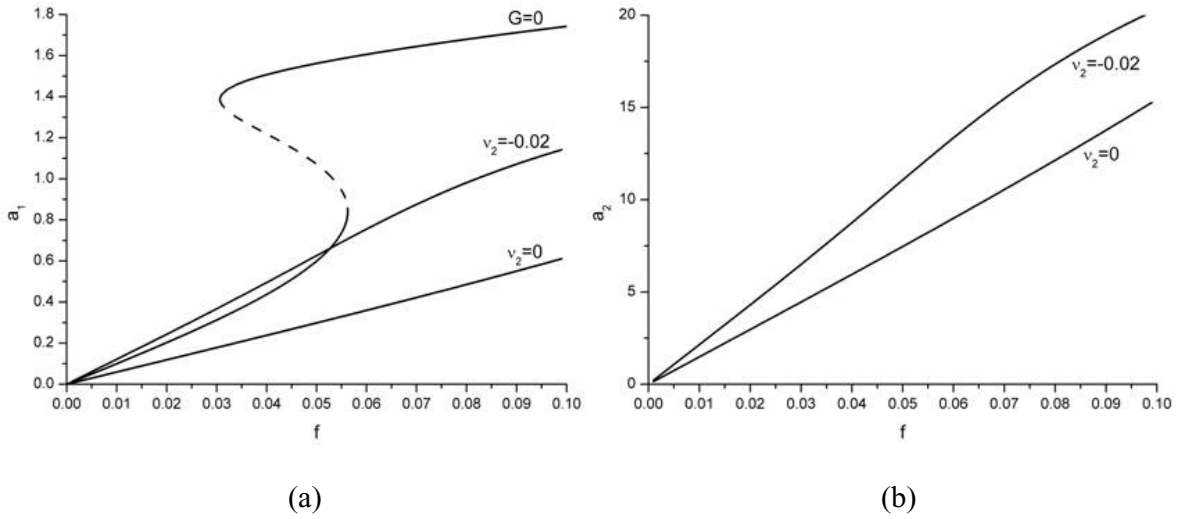

Fig. 14. Effect of detuning the absorber's frequency on the force-response curves of (a) the plant and (b) the absorber when $\sigma_1 = -0.1$, $G = 0.01$ and $\zeta = 0.02$.

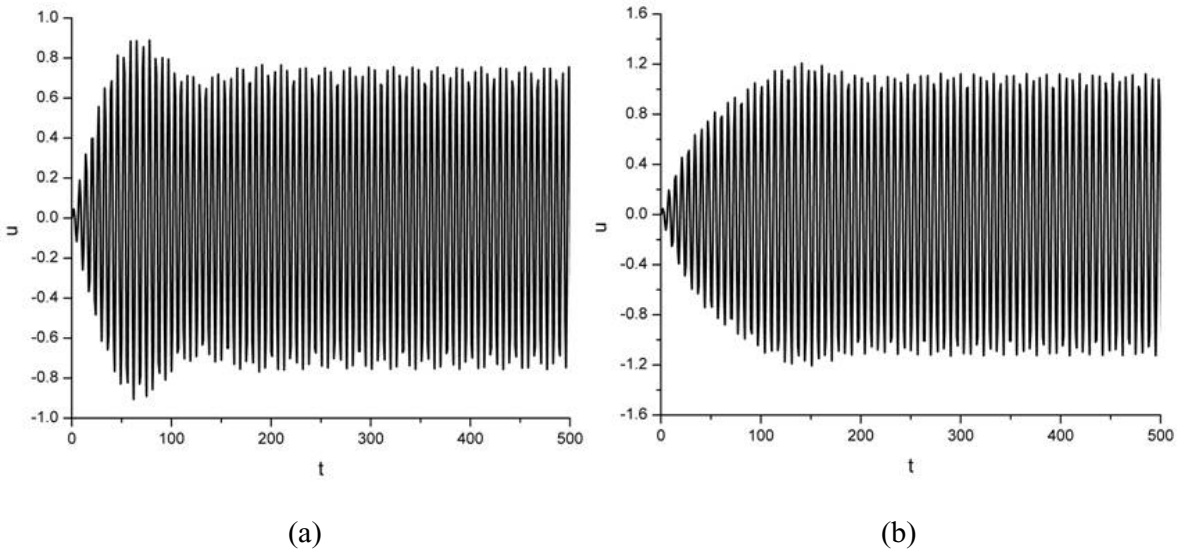

Fig. 15. Numerical simulation of the time responses of the plant for the open-loop case when (a) $\Omega = 1.0$ and (b) $\Omega = 0.95$.

$$\ddot{v} + 2\zeta\dot{v} + \omega_2^2 v = \omega_2^2 u \tag{21}$$

where $\mu_1 = 0.01$, $\mu_2 = 0.02$, $\alpha_3 = -0.08$, $\delta = 0.08$, $\eta_1 = 2$, $\omega_1 = 1$, $\zeta = 0.02$, $\tau_e = 0$ and $f = 0.025$. The numerical simulations are performed for different values of the absorber's frequency ω_2, the forcing frequency Ω and the feedback gain G. Zero initial conditions, i.e., $u(0) = 0$, $\dot{u}(0) = 0$, $v(0) = 0$ and $\dot{v}(0) = 0$, are chosen for all the numerical simulations. The time responses of the plant for the open-loop case when $\Omega = 1.0$ and $\Omega = 0.95$ are shown in Fig. 15. The time responses of the plant and the absorber when $\omega_2 = 1.0$ and $\Omega = 1.0$ (i.e., $\sigma_1 = 0$, $\nu_2 = 0$) for $G = 0.005$ and $G = 0.01$ are shown in Figs 16 and 17. The time responses of the plant and the absorber when $\omega_2 = 0.95$ and $\Omega = 0.95$ (i.e., $\sigma_1 = -0.05$, $\nu_2 = 0$) for $G = 0.005$ and $G = 0.01$ are shown in Figs 18 and 19. The time responses of the plant and the absorber when $\omega_2 = 0.97$ and $\Omega = 0.95$ (i.e., $\sigma_1 = -0.05$, $\nu_2 = -0.02$) for $G = 0.005$ and $G = 0.01$ are shown in Figs 20 and 21. Comparing Figs 6–7 and Figs 16–21, it can be seen

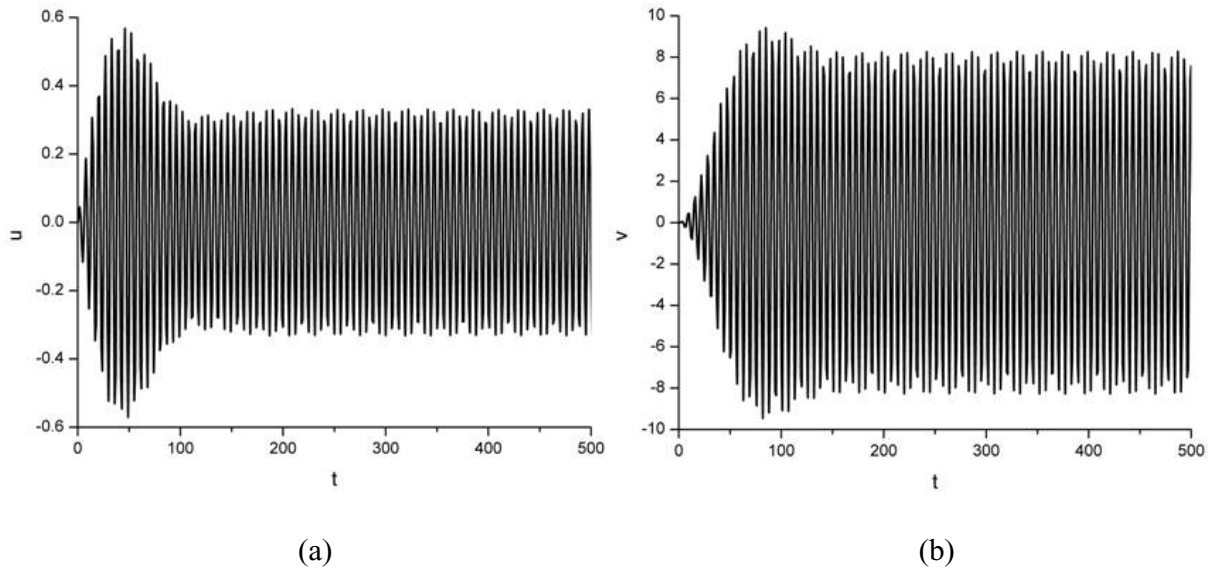

Fig. 16. Numerical simulation of the time response of (a) the plant and (b) the absorber when $\omega_2 = 1.0$, $\Omega = 1.0$ and $G = 0.002$.

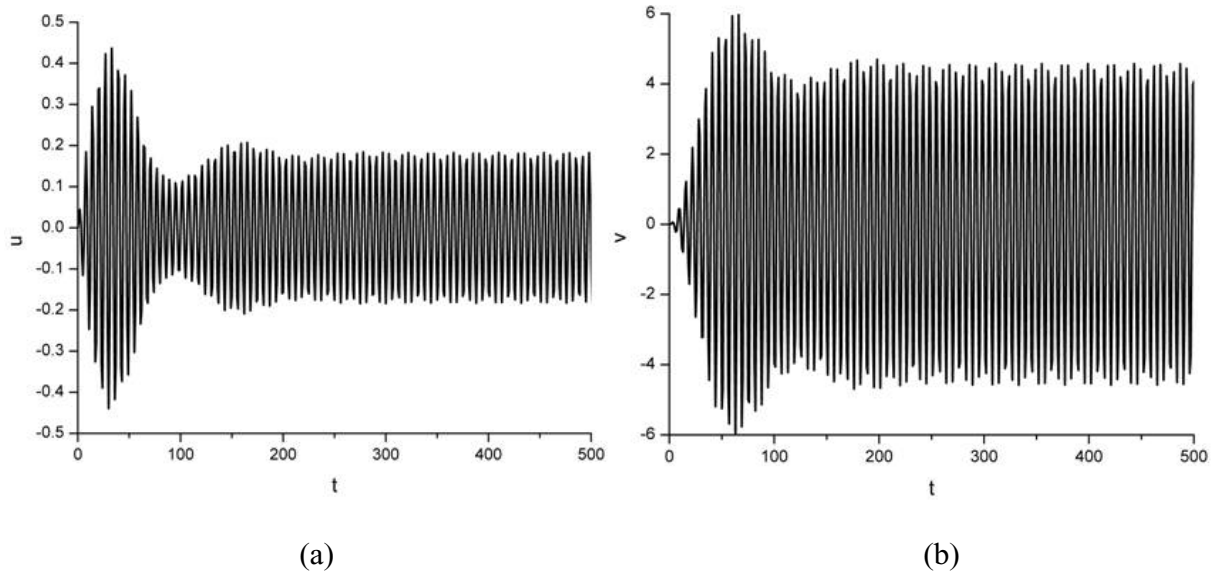

Fig. 17. Numerical simulation of the time response of (a) the plant and (b) the absorber when $\omega_2 = 1.0$, $\Omega = 1.0$ and $G = 0.01$.

that the response amplitudes predicted by the perturbation solution are in good agreement with the results of the numerical simulations. The results of numerical simulations shown in Figs 15–21 also indicate that large amplitude of the plant can be reduced by introducing PPF control strategy.

6. Conclusions

An active linear absorber based on PPF control is used to suppress the high-amplitude vibration of the single-mode of the flexible beam when subjected to primary resonance excitation. The method of multiple scales is used to derive

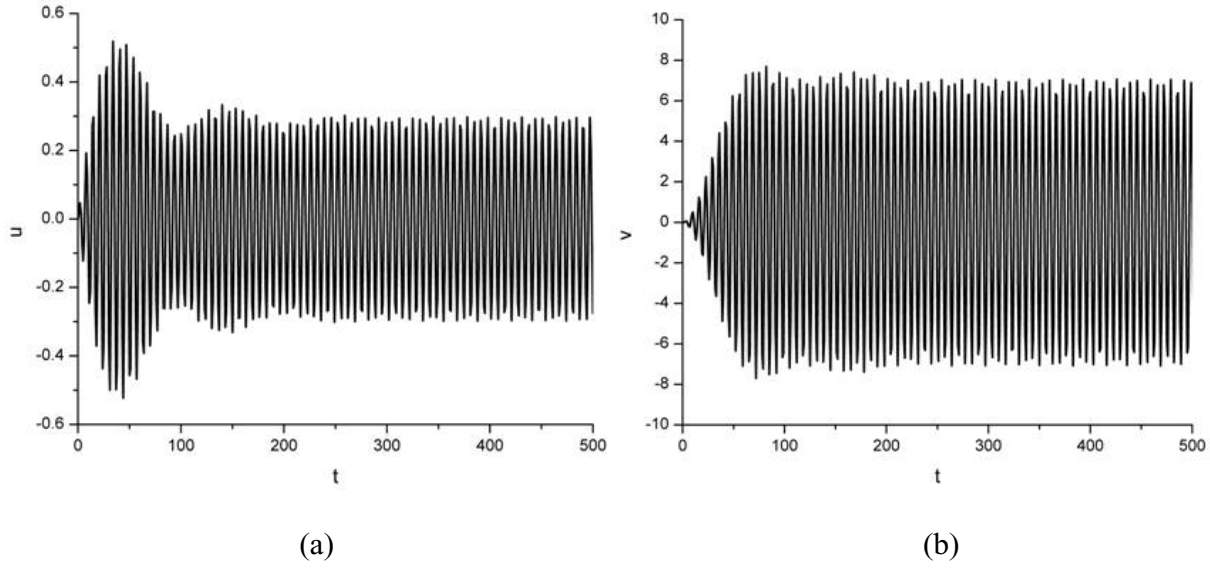

Fig. 18. Numerical simulation of the time response of (a) the plant and (b) the absorber when $\omega_2 = 0.95$, $\Omega = 0.95$ and $G = 0.002$.

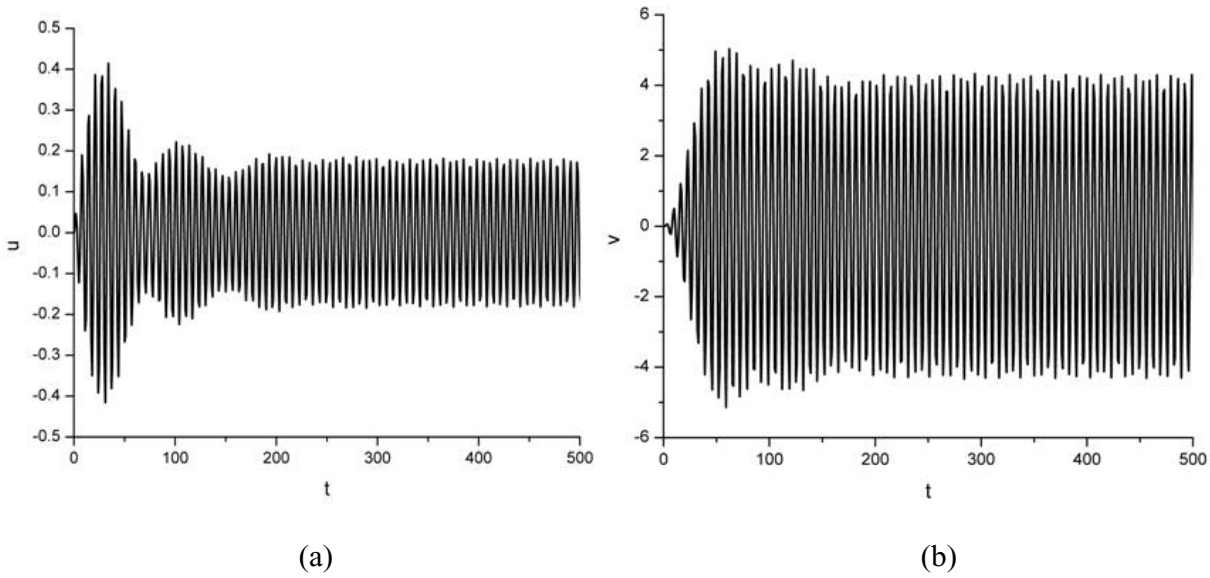

Fig. 19. Numerical simulation of the time response of (a) the plant and (b) the absorber when $\omega_2 = 0.95$, $\Omega = 0.95$ and $G = 0.01$.

four first-order differential equations governing the amplitudes and phases of the responses. Then a bifurcation analysis is conducted to examine the stability of the system and the performance of the control law is investigated. Also, a parametric investigation is carried out to examine the effects of the damping ratio of the absorber, the value of the feedback gain and detuning frequency of the absorber on the responses. Finally, the perturbation solutions are validated by the results from direct numerical integration.

With the absorber's frequency being tuned to the excitation frequency, as the feedback gain increases, the response amplitudes of both the plant and the absorber decrease; as the absorber's damping decreases, the response amplitude of the plant reduces at the expense of increasing the response amplitude of the absorber. However, this is not the fact for the case of absorber's frequency detuning from the excitation frequency, as the feedback gain increases,

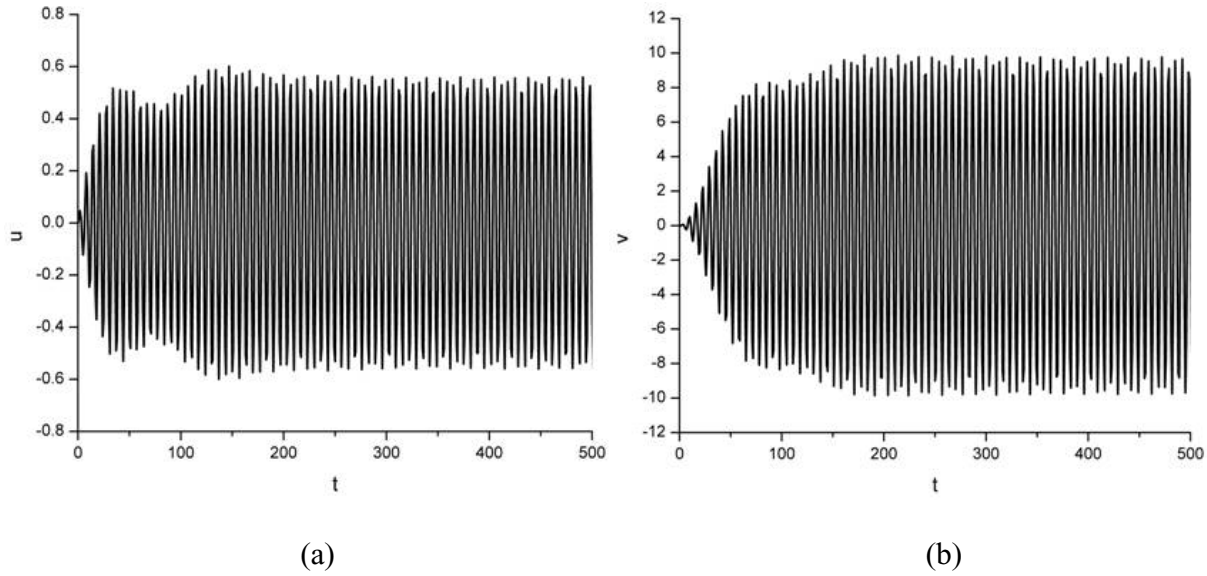

(a) (b)

Fig. 20. Numerical simulation of the time response of (a) the plant and (b) the absorber when $\omega_2 = 0.97$, $\Omega = 0.95$ and $G = 0.002$.

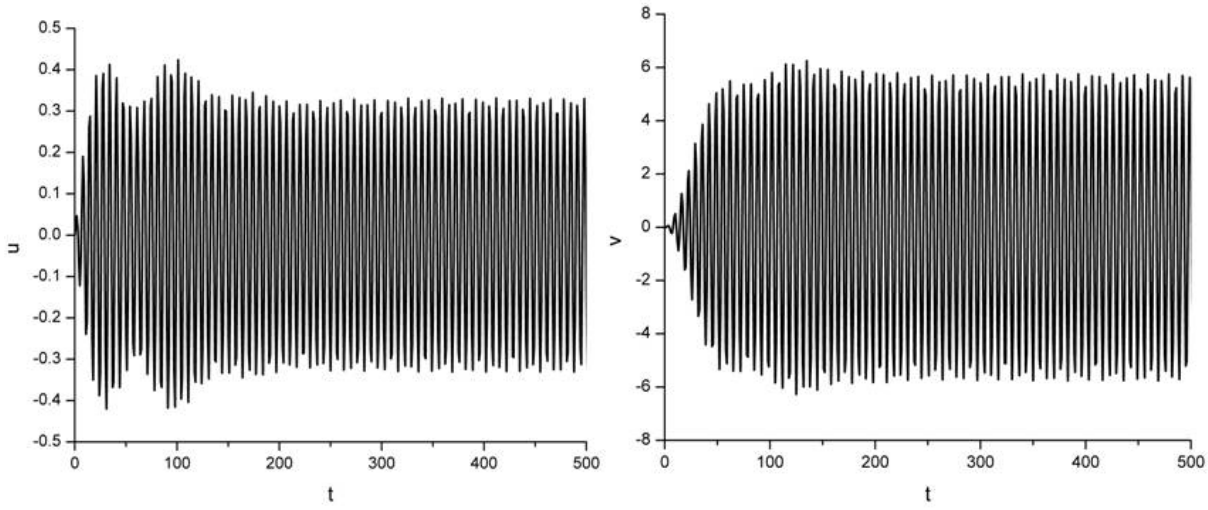

(a) (b)

Fig. 21. Numerical simulation of the time response of (a) the plant and (b) the absorber when $\omega_2 = 0.97$, $\Omega = 0.95$ and $G = 0.01$.

although the maximum response amplitudes of both the plant and the absorber decrease, in certain frequency region the response amplitudes of both the plant and the absorber increase; as the absorber's damping decreases, not only the maximum response amplitude of the plant but also the response amplitude of the absorber increase. It also should be mentioned that the response of the plant degrades when the absorber's frequency detuning from the excitation frequency.

Acknowledgements

The author desires to express his thanks to reviewers for their valuable suggestions.

References

[1] H. Hu, E.H. Dowell and L.N. Virgin, Resonances of a harmonically forced Duffing oscillator with time delay state feedback, *Nonlinear Dynamics* **15** (1998), 311–327.

[2] A.A. El-Badawy and A.H. Nayfeh, Control of a directly excited structural dynamic model of an F-15 tail section, *Journal of the Franklin Institute* **338** (2001), 133–147.

[3] O.C. Pinto and P.B. Goncalves, Active non-linear control of buckling and vibrations of a flexible buckled beam, Chaos, *Solitons and Fractals* **14** (2002), 227–239.

[4] A. Maccari, Vibration control for the primary resonance of the van der Pol oscillator by a time delay state feedback, *International Journal of Nonlinear Mechanics* **38** (2003), 123–131.

[5] A.F. El-Bassiouny, Single-mode control and chaos of cantilever beam under primary and principal parametric excitations, Chaos, *Solitons and Fractals* **30** (2006), 1098–1121.

[6] J. Li, R. Shen and H. Hua, Cubic velocity feedback control of high-amplitude vibration of a nonlinear plant to a primary resonance excitation, *Shock and Vibration* **14** (2007), 1–14.

[7] C.J. Goh and T.K. Caughey, On the stability problem caused by finite actuator dynamics in the collocated control of large space structures, *International Journal of Control* **41** (1985), 787–802.

[8] J.N. Juang and M. Phan, Robust controller designs for second order dynamic systems: a virtual passive approach, *Journal of Guidance, Control, and Dynamics* **15** (1992), 1192–1198.

[9] J.L. Fanson and T.K. Caughey, Positive position feedback control for large space structures, *AIAA Journal* **28** (1990), 717–724.

[10] L. Meirovitch, H. Baruh and H. Oz, Comparison of control techniques for large flexible systems, *Journal of Guidance and Control* **6** (1983), 302–310.

[11] T.K. Caughey, Dynamic response of structures constructed from smart materials, *Smart Materials and Structures* **4** (1995), A101–A106.

[12] A. Baz and J.T. Hong, Adaptive control of flexible structures using modal positive position feedback, *International Journal of Adaptive Control and Signal Processing* **11** (1997), 231–253.

[13] P.F. Pai, B. Wen, A.S. Naser and M.J. Schulz, Structural vibration control using PZT patches and non-linear phenomena, *Journal of Sound and Vibration* **215** (1998), 273–296.

[14] M.I. Friswell and D.J. Inman, The relationship between positive position feedback and output feedback controllers, *Smart Materials and Structures* **8** (1999), 285–291.

[15] G. Song, S.P. Schmidt and B.N. Agrawal, Experimental robustness study of positive position feedback control for active vibration suppression, *Journal of Guidance, Control, and Dynamics* **25** (2002), 179–182.

[16] G. Song, P.Z. Qiao, W.K. Binienda, G.P. Zou, Active Vibration Damping of Composite Beam using Smart Sensors and Actuators, *Journal of Aerospace Engineering* **15**(3) (2002), 97–103.

[17] K.H. Rew, J.H. Han and I. Lee, Multi-modal vibration control using adaptive positive position feedback, *Journal of Intelligent Material Systems and Structures* **13** (2002), 13–22.

[18] J. Shan, H.T. Liu and D. Sun, Slewing and vibration control of a single-link flexible manipulator by positive position feedback (PPF), *Mechatronics* **15** (2005), 487–503.

[19] P. Shimon, E. Richer and Y. Hurmuzlu, Theoretical and experimental study of efficient control of vibrations in a clamped square plate, *Journal of Sound and Vibration* **282** (2005), 453–473.

[20] Z. Qiu, X. Zhang, H. Wu and H. Zhang, Optimal placement and active vibration control for piezoelectric smart flexible cantilever plate, *Journal of Sound and Vibration* **301** (2007), 521–543.

[21] L. Chen, C.H. Hansen, F. He and K. Sammut, Active nonlinear vibration absorber design for flexible structures, *International Journal of Acoustics and Vibration* **12** (2007), 51–59.

[22] M.K. Kwak and S. Heo, Active vibration control of smart grid structure by multiinput and multioutput positive position feedback controller, *Journal of Sound and Vibration* **304** (2007), 230–245.

[23] L.D. Zavodney and A.H. Nayfeh, The nonlinear response of a slender beam carrying a lumped mass to a principal parametric excitation: theory and experiment, *International Journal of Nonlinear Mechanics* **24** (1989), 105–125.

[24] A.H. Nayfeh and B. Balachandran, *Applied Nonlinear Dynamics*, Wiley, New York, 1995.

[25] L. Meirovitch, *Dynamics and Control of Structures*, Wiley, New York, 1990.